Bulletin of the Seismological Society of America, Vol. 92, No. 8, pp. 2946–2960, December 2002

Puente Hills Blind-Thrust System, Los Angeles, California

by John H. Shaw, Andreas Plesch, James F. Dolan, Thomas L. Pratt, and Patricia Fiore

Abstract We describe the three-dimensional geometry and Quaternary slip history of the Puente Hills blind-thrust system (PHT) using seismic reflection profiles, petroleum well data, and precisely located seismicity. The PHT generated the 1987 Whittier Narrows (moment magnitude [M_w] 6.0) earthquake and extends for more than 40 km along strike beneath the northern Los Angeles basin. The PHT comprises three, north-dipping ramp segments that are overlain by contractional fault-related folds. Based on an analysis of these folds, we produce Quaternary slip profiles along each ramp segment. The fault geometry and slip patterns indicate that segments of the PHT are related by soft-linkage boundaries, where the fault ramps are en echelon and displacements are gradually transferred from one segment to the next. Average Quaternary slip rates on the ramp segments range from 0.44 to 1.7 mm/yr, with preferred rates between 0.62 and 1.28 mm/yr. Using empirical relations among rupture area, magnitude, and coseismic displacement, we estimate the magnitude and frequency of single (M_w 6.5–6.6) and multisegment (M_w 7.1) rupture scenarios for the PHT.

Introduction

The Los Angeles basin lies along the southern California coast at the junction of the Transverse and Peninsular Ranges. The basin is currently being deformed by several blind-thrust and strike-slip faults that have generated historic, moderate-size earthquakes (Hauksson, 1990; Dolan *et al.*, 1995). Geodetic studies suggest that the northern basin is shortening at a rate of 4.4–5 mm/yr in a north–south to northeast–southwest direction (Walls *et al.*, 1998; Argus *et al.*, 1999; Bawden *et al.*, 2001). Part of this shortening is accommodated on recognized fault systems, and two competing models have been proposed to explain which faults account for the remainder. Walls *et al.* (1998) suggested that the remaining shortening is accommodated by higher rates of slip on conjugate strike-slip systems in the northern basin. Motion on these faults produces north–south shortening by lateral crustal extrusion. In contrast, Argus *et al.* (1999) and Bawden *et al.* (2001) proposed that the shortening is accommodated primarily by activity on thrust and reverse faults. In this article, we document an active blind-thrust system in the northern Los Angeles basin, termed the Puente Hills blind thrust (PHT), that accommodates a component of the unresolved basin shortening and poses substantial earthquake hazards to metropolitan Los Angeles.

The PHT extends for more than 40 km along strike in the northern Los Angeles basin from downtown Los Angeles east to Brea in northern Orange County (Fig. 1). The fault consists of at least three distinct geometric segments, termed Los Angeles, Santa Fe Springs, and Coyote Hills, from west to east. Shaw and Shearer (1999) defined the central portion of the PHT with seismic reflection profiles and petroleum well data. Using precisely relocated seismicity, these authors proposed that the Santa Fe Springs segment of the PHT generated the 1987 (M_w 6) Whittier Narrows earthquake. In this article, we define the size and three-dimensional geometry of the PHT using additional seismic reflection data. We describe the systematic behavior of the segments that compose the PHT and consider the geometric and kinematic relations of the PHT to other blind-thrust and strike-slip systems. Finally, we map the distribution of slip on the PHT and discuss the implications of this study for earthquake hazard assessment in metropolitan Los Angeles.

Puente Hills Blind Thrust

Displacements on the PHT contribute to the growth of a series of en echelon anticlines in the northern Los Angeles basin that involve Miocene through Quaternary strata. The easternmost fold forms the Coyote Hills and provides structural closure for the east and west Coyote Hills oil fields (Yerkes, 1972). The central fold has only subtle surface expression and provides structural closure for the Santa Fe Springs oil field (Fig. 1). The westernmost fold is contained within a broad, south-dipping monocline that forms the northern boundary of the Los Angeles basin (Davis *et al.*, 1989; Shaw and Suppe, 1996; Schneider *et al.*, 1996). All of these folds are bounded on their southern margins by narrow forelimbs (Fig. 2). These forelimbs, or kink bands, consist of concordantly folded, south-dipping Pliocene

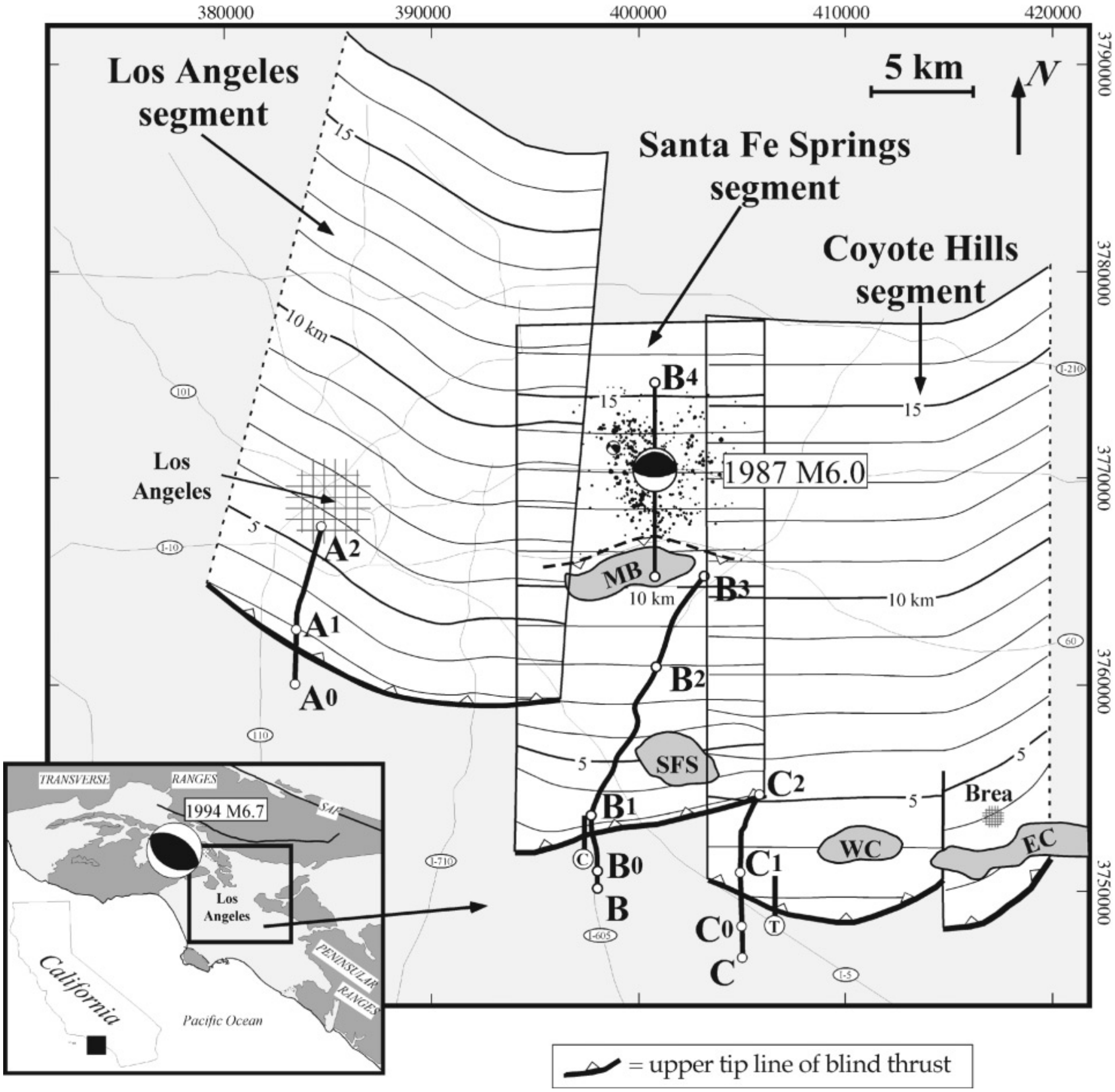

Figure 1. Structure contour map of segments of the Puente Hills blind thrust (PHT) showing the location of the 1987 Whittier Narrows (M_w 6) earthquake sequence (Hauksson and Jones, 1989) as relocated by Shaw and Shearer, (1999). A^0–A^2, B–B^4, and C–C^2 mark the traces of seismic reflection profiles and cross sections shown in Figures 2, 3, 5, 7, and 8. Traces T and C correspond to the high-resolution seismic profiles presented in Figure 4. The inset shows the location of the PHT and 1994 Northridge (M_w 6.7) earthquake. Oil fields: EC, East Coyote; WC, West Coyote; SFS, Santa Fe Springs; MB, Montebello. Major state and interstate highways are shown for reference. Map coordinates are UTM Zone 11, NAD27 datum.

strata. Overlying upper Pleistocene and younger units thin across these folds, suggesting that they were deposited concurrent with fold growth and fault activity (Yerkes, 1972; Myers, 2001). The kink bands generally narrow upward into this upper Pleistocene and younger section, forming growth triangles. These growth structures are diagnostic of fault bend and certain types of tip line or fault propagation folding (Suppe *et al.*, 1992; Shaw and Suppe, 1994; Allmendinger, 1998).

The PHT and overlying folds are imaged in a set of 43 seismic reflection profiles available for this study that were acquired by the petroleum industry along roads, rivers, and utility rights of way in the northern basin. The PHT is expressed directly in 24 of these profiles as a series of north-dipping reflections that extend downward from the base of the forelimb kink bands beneath the cores of the anticlines. Based on velocity functions derived from more than 150 sonic logs and 7000 stacking velocity measurements (Süss

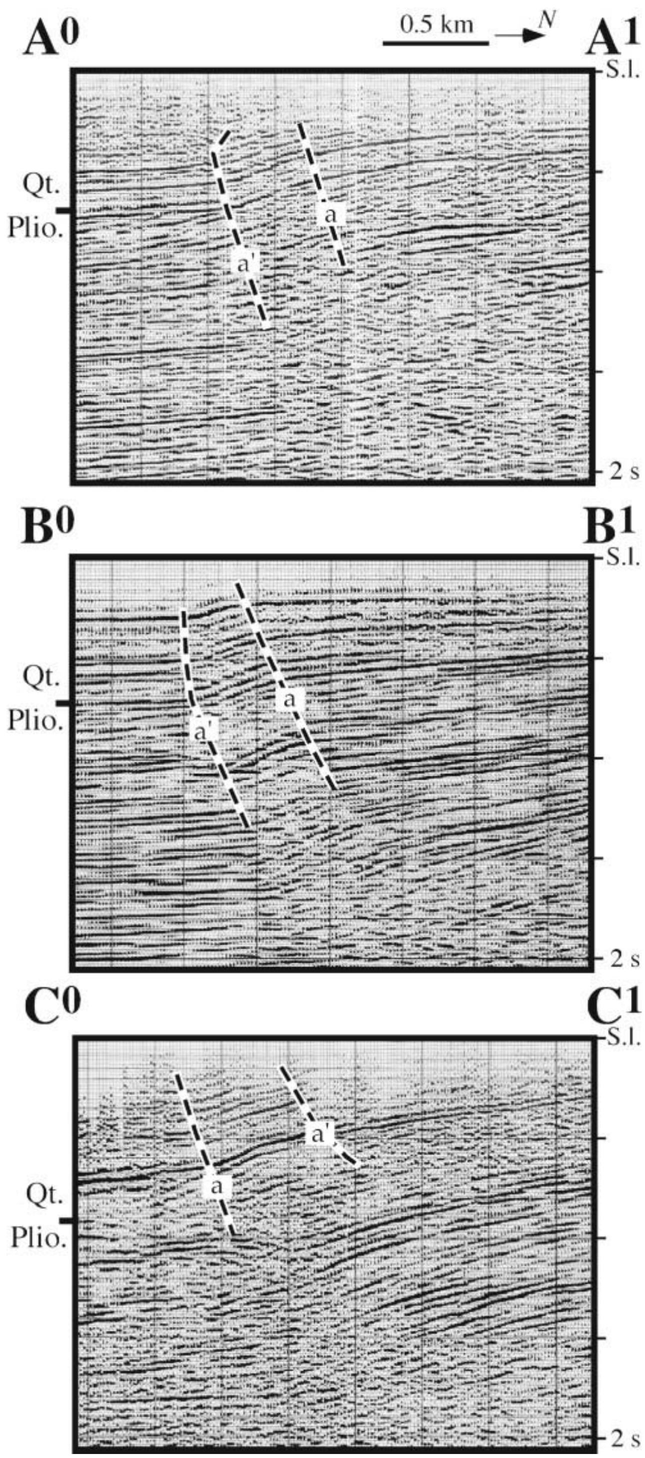

Figure 2. Migrated seismic reflection profiles across the forelimb kink bands (aa′) that mark the southern termination of the Los Angeles (A^0–A^1), Santa Fe Springs (B^0–B^1), and Coyote (C^0–C^1) segments of the Puente Hills blind thrust. The fold limbs are overlain by Quaternary growth strata that thin to the north onto the crests of the structures. Profile traces are shown in Figure 1.

and Shaw, 2002), the seismic data were depth converted revealing that the fault-plane reflections dip to the north at 25° to 30°. A structure contour map based on the fault-plane reflections indicates that the PHT strikes generally east–west, and that it is composed of three distinct geometric segments termed Coyote Hills, Santa Fe Springs, and Los Angeles (Shaw and Shearer, 1999). This en echelon fault pattern mimics the trend of the overlying folds.

Santa Fe Springs Segment

The best-imaged portion of the PHT lies beneath the Santa Fe Springs anticline, where fault-plane reflections extend from about 3- to more than 7 km depth (Fig. 3). The thrust ramp dips to the north at about 25°–29° and terminates upward at the base of the forelimb kink band (aa′) on the southern margin of the fold. To the north of this kink band is located a second, apparently older hanging-wall fold defined by anticlinal axial surface (c) and a steeply southwest-dipping fold limb (Fig. 3). A gently southwest-dipping monoclinal fold also underlies the PHT. This footwall structure has been interpreted to reflect deformation above the lower Elysian Park thrust (Shaw and Suppe, 1996).

In contrast to the shallow, tight kink-band (aa′), the northern hanging-wall fold (c) in the Santa Fe Springs anticline is broad and open (Fig. 3). Thinning of strata across this northern limb suggests that it formed in the Pliocene during an early stage of activity on the PHT. Allmendinger and Shaw (2000) modeled this Pliocene structure as a trishear fault-propagation fold (Erslev, 1991; Allmendinger, 1998) and showed that the fold shape was consistent with the imaged fault geometry. Late Pliocene (uppermost Fernando Fm.) and Quaternary strata overlie but are not involved in this broad fold limb, suggesting that this portion of the structure stopped growing in the late Pliocene. A period of tectonic quiescence is defined by a 500-m-thick section of late Pliocene strata that does not change thickness across the forelimb of the Santa Fe Springs structure (Fig. 3). In the Quaternary, the narrow kink band (aa′) formed on the south margin of the fold, likely representing upward and southward propagation (reactivation) of this segment of the PHT.

The Quaternary growth structure of kink band aa′ exhibits an active anticlinal axial surface (a) that extends to the upper limit of industry seismic reflection profiles at about 300-m depth, and an inactive synclinal axial surface (a′) that bounds the other side of the growth triangle (Fig. 3) (Suppe *et al.*, 1992). High-resolution seismic reflection profiles acquired across the structure (Carfax site, Fig. 4) image the fold extending upward from 400 to ~25-m depth (Pratt *et al.*, 2002). Deformation of shallow, late Quaternary deposits is localized above the active, anticlinal axial surface. This growth geometry is consistent with development of the kink band by fault-bend folding (Suppe *et al.*, 1992; Shaw and Suppe, 1996; Pratt *et al.*, 2002) as the PHT flattens to an upper detachment in the central Los Angeles basin (Fig. 5). This interpretation implies that small amounts of displace-

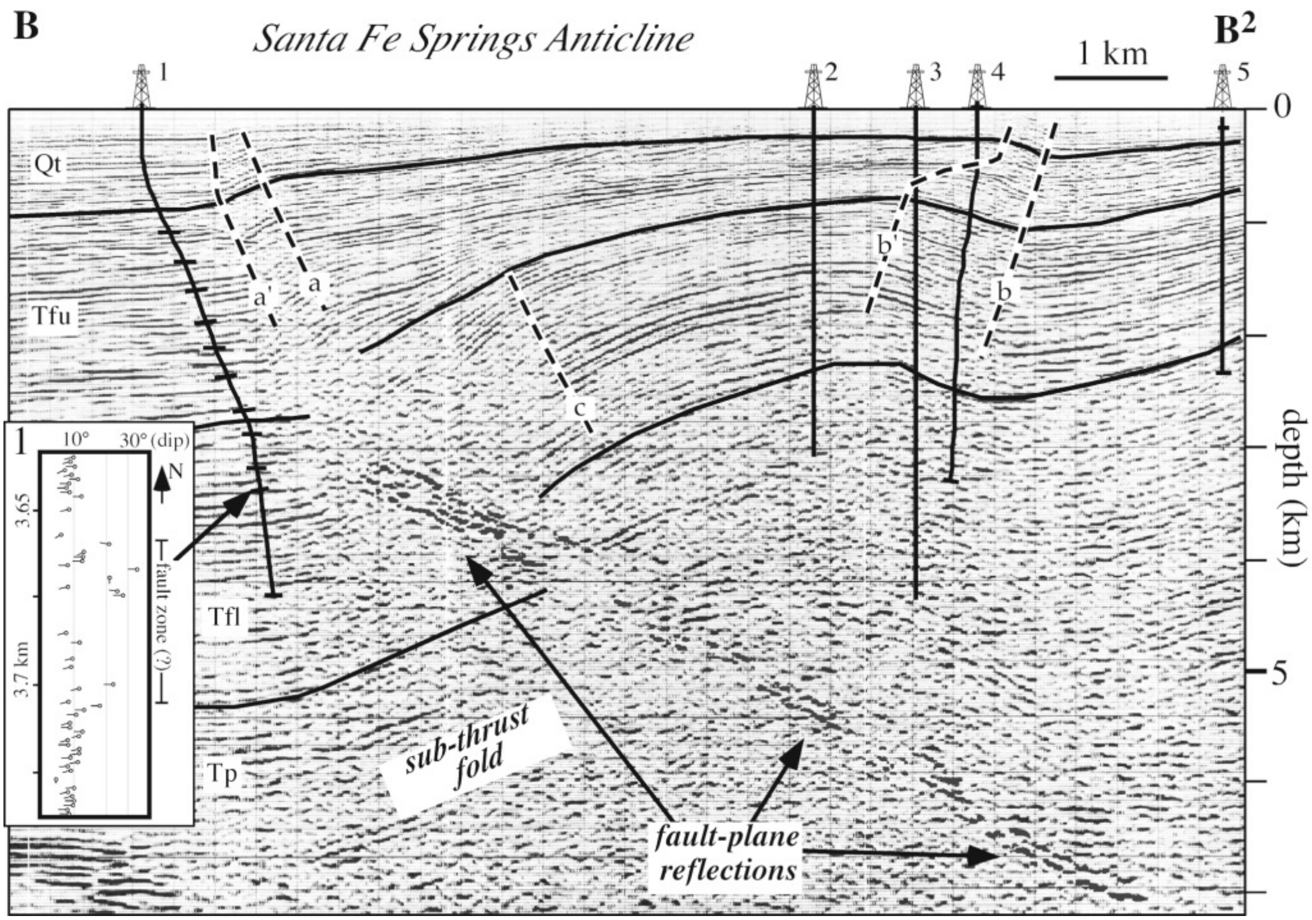

Figure 3. Migrated and depth converted seismic reflection profile across the Santa Fe Springs segment of the PHT after Shaw and Shearer (1999). The fold is bounded by kink bands (aa′; bb′) that narrow upward, forming growth triangles in the Quaternary section. The fault was interpreted and highlighted using an automated tracking technique that correlates reflections based on amplitude and lateral coherence within a given region and dip range. The inset shows a zone of chaotic bed dips at the interpreted upper detachment level in dipmeter log from the Union Bellflower #2 well. Profile traces are shown in Figure 1. Qt, Quaternary; Tfu, Pliocene upper Fernando Formation; Tfl, Pliocene lower Fernando Formation; Tp, Miocene Puente Formation. Wells: 1, Union Bellflower #2; 2, Chevron Newsome Community #1; 3, Chevron Houghton Community #1; 4, Conoco Felix #1; 5, Exxon Whittier #1.

ment (≤ 500 m) extend southward on this upper detachment into the central Los Angeles basin. The proposed detachment level is penetrated by the Union Bellflower #2 well (Fig. 3), which encountered a zone of chaotic dips at this location in an otherwise monotonous, gently southwest-dipping section.

The proposed multistage structural history of the Santa Fe Springs segment of the PHT is also recorded in the growth structure on the back limb of the anticline (Fig. 6). This structure contains another growth triangle. In contrast to the forelimb kink band, however, the backlimb growth triangle contains an active synclinal axial surface (b) and an inactive anticlinal axial surface (b′). This geometry is consistent with the backlimb structure forming above a subtle, steepening-upward bend in the PHT. Consistent with the forelimb interpretation, the backlimb growth structure defines a middle Pliocene phase of fold growth, followed by late Pliocene tectonic quiescence and a Quaternary period of reactivation.

The contoured fault-plane reflections define an east–west striking, 25°–29° N dipping Santa Fe Springs segment of the PHT (Fig. 1). Shaw and Shearer (1999) noted that this orientation matched the preferred nodal plane of the 1987 Whittier Narrow (M_w 6.0) earthquake (Hauksson and Jones, 1989). Using L-1 norm waveform cross-correlation techniques (Shearer, 1997) and velocity data derived from sonic logs, Shaw and Shearer (1999) relocated the earthquake and its aftershocks. The relocated cluster defined the dip of the preferred nodal plane and was positioned directly at the down-dip extension of the PHT imaged in the seismic reflection data (Fig. 5). This led Shaw and Shearer (1999) to conclude that the 1987 Whittier Narrows earthquake rup-

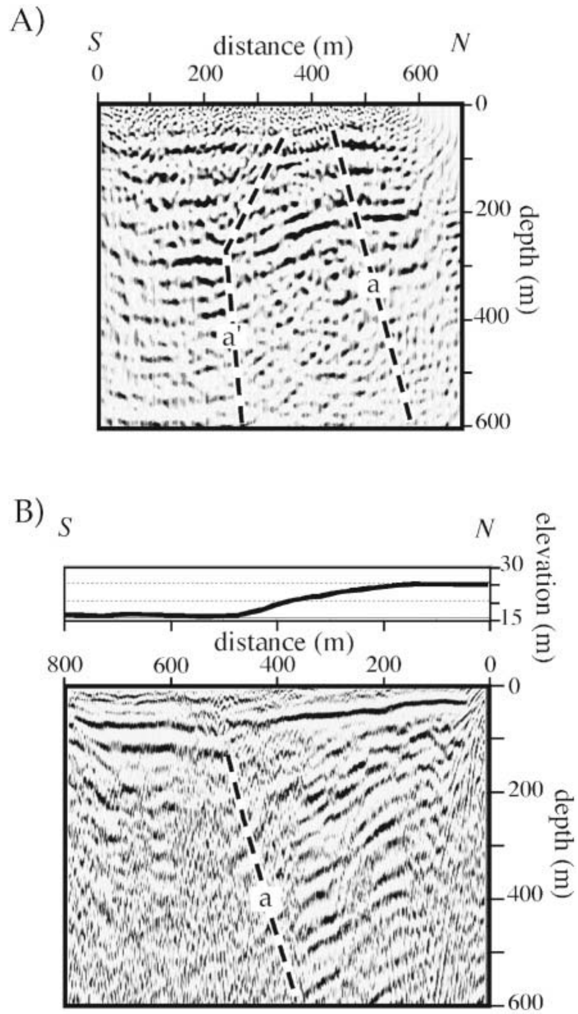

Figure 4. High-resolution seismic reflection profiles acquired with hammer drop and Mini-Sosie (Barbier, 1983) sources across the forelimbs that overlie the Santa Fe Springs (A, Carfax site) and Coyote Hills (B, Trojan Way site) segments of the PHT (Pratt *et al.*, 2002). Deformed strata corresponding to reflections in the shallow subsurface define late Quaternary activity on the PHT. Deformation is localized along active (a) axial surfaces, which correspond to the axial surfaces imaged in the industry reflection profile (Fig. 3, 6). Profile traces (C, Carfax; T, Trojan Way) are shown in Figure 1.

tured a small patch (~30 km^2) of the Santa Fe Springs segment of the PHT, demonstrating the activity and seismogenic potential of this blind-thrust system.

Coyote Hills Segment

The Coyote Hills segment of the PHT is defined by fault-plane reflections and reflection truncations in seismic profiles between 2- and 5-km depth beneath the western Coyote Hills anticline (Figs. 2, 6). Similar to the Santa Fe Springs structure, the Coyote Hills anticline is a broad, open fold bounded on its southern margin by a discrete forelimb kink band (aa′) that contains parallel, south-dipping (15°–30°) Pliocene strata. The fault extends upward to the base of this kink band, which is underlain by horizontal, relatively undeformed Miocene strata. Quaternary strata thin above this kink band in an apparent growth triangle, defining the age of fold growth and activity of the Coyote Hills thrust. This growth period initiates at a seismic sequence boundary that correlates with the beginning of the Quaternary growth phase on the Santa Fe Springs structure. In contrast to the Santa Fe Springs structure, however, the Coyote Hills kink band appears to contain an active synclinal axial surface (a) and an inactive anticlinal axial surface (a′) (Fig. 7). These observations are consistent with the fold geometry imaged in a high-resolution, Mini-Sosie profile (Trojan Way site, Fig. 4), which shows late Quaternary deformation localized above the synclinal axial surface (Pratt *et al.*, 2002). The syncline also corresponds with a surface fold scarp. This geometry is consistent with slip on the Coyote Hills thrust being entirely consumed in the kink band by some type of tip-line (fault-propagation) folding process (Suppe and Medwedeff, 1990; Allmendinger, 1998). Alternatively, the Coyote Hills thrust may shallow to an upper detachment from which a backthrust emanates, forming a structural wedge (Medwedeff, 1992).

A second, older seismic reflection survey images the Eastern Coyote anticline, including the steep kink band on the southern margin of the fold (Fig. 1). The older data, however, do not provide a direct image of the fault surface. We extrapolate the PHT beneath the Eastern Coyote Hills using the relationship between the fold and fault defined in the Western Coyote Hills. This includes positioning the fault at the base of the forelimb kink band as well as defining the dip of the fault as a function of bedding dip in the forelimb kink band. This yields a relatively simple, planar surface for the PHT beneath the Eastern Coyote Hills that dips to the north-northwest at about 25–30°. The strike of this fault segment mimics that of the Eastern Coyote Hills anticline, which is about N60°E (Wright, 1991), in contrast to the east–west strike of the Western Coyote Hills (Fig. 1). The fold geometries and the change in strikes imply that there is a shallow offset between the thrust ramps underlying the Western and Eastern Coyote Hills. When these two fault surfaces are projected to depth using a smoothed average of their dips, they intersect at relatively shallow crustal levels (~5 km). This suggests that the Eastern and Western Coyote Hills segment merge to a common basal ramp at this depth (Fig. 1). Alternatively, the fault segments may crosscut one another.

Based on our projections, the ramps of the Coyote Hills and Santa Fe Springs segments are separated by only a few hundred meters at depths below 8 km (Fig. 1). Thus, it is possible that these segments merge at depth to form a single, continuous ramp.

Los Angeles Segment

The Los Angeles segment of the PHT extends from the western margin of the Montebello Hills to about 5 km west

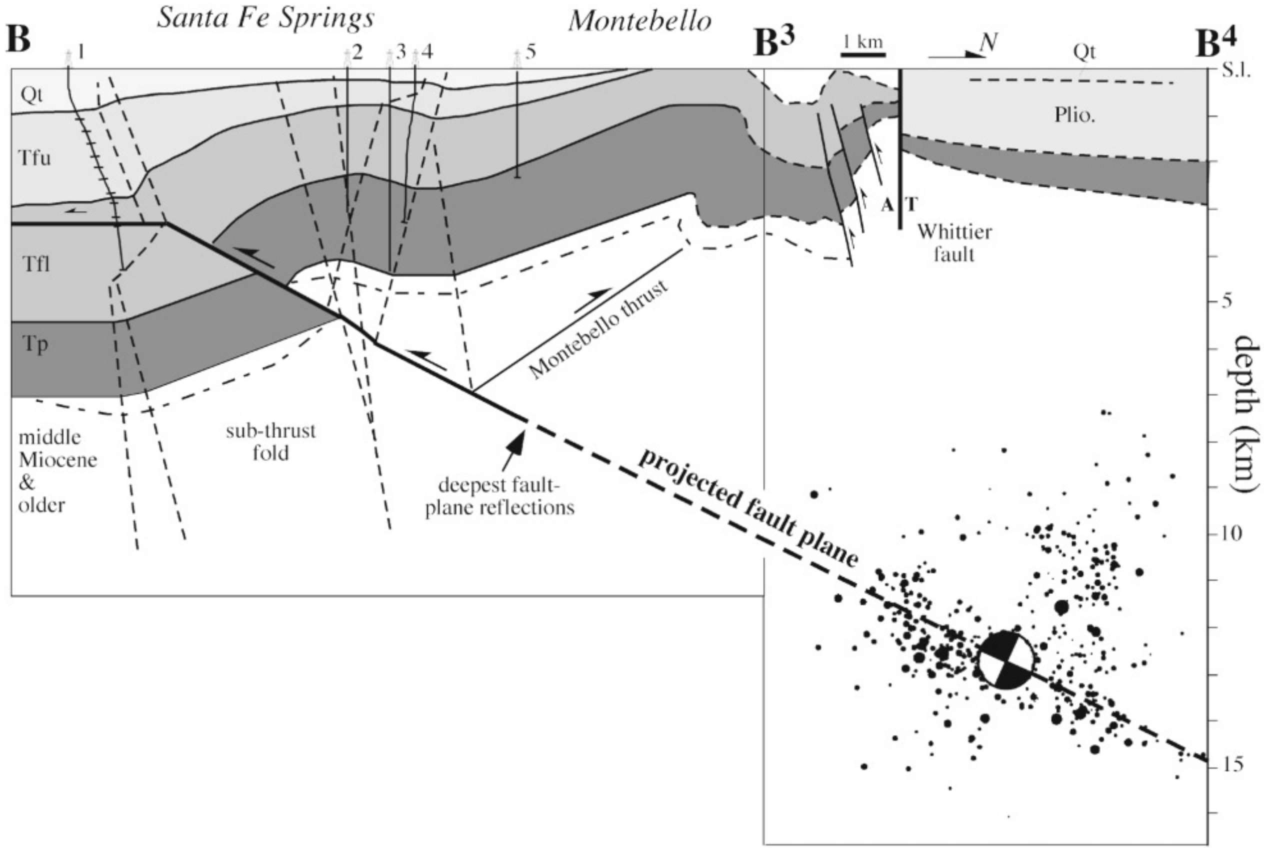

Figure 5. Geologic cross section showing relation of the Santa Fe Springs segment of the PHT to the hypocenters of the 1987 Whittier Narrows (M_w 6) earthquake and aftershocks after Shaw and Shearer (1999). The hypocenters were relocated by Shaw and Shearer (1999) using L-1 norm waveform cross-correlation techniques (Shearer, 1997) and velocity control from nearby oil wells. Profile trace is shown in Figure 1. Section B–B^3 is based on the seismic profile shown in Figure 3; section B^3–B^4 is based on Wright (1991). The subthrust fold is related to the lower Elysian Park trend of Davis *et al.* (1989). Formation symbols identified in caption for Figure 3.

of downtown Los Angeles (Fig. 1), which represents the westernmost extent of our seismic reflection data. The fold consists of a narrow kink band with south-dipping strata superimposed on a gently south-dipping monocline that forms the northern boundary of the central Los Angeles basin (Figs. 2, 8). Precise definition of the age of the kink band is difficult, as the section is poorly imaged above the base Quaternary sequence boundary that marks the initiation of growth in the Santa Fe Springs and Coyote structures (Fig. 2). Nevertheless, the Los Angeles segment kink band developed no earlier than this base Quaternary sequence boundary, as underlying upper Pliocene strata do not change thickness across the structure. In contrast, Quaternary strata thin above the structure. Thus, the kink band appears to have developed in the Quaternary, contemporaneous with the Santa Fe Springs and Coyote structures.

The Los Angeles segment of the PHT is defined by fault-plane reflections and reflection truncations at the base of the forelimb kink band in both north–south (Fig. 8) and east–west trending seismic profiles. In the eastern portion of the Los Angeles segment, the thrust ramp strikes east–west, generally parallel to the Santa Fe Springs and Western Coyote fault segments (Fig. 1). The western two-thirds of the Los Angeles segment, however, strike roughly N60°W. This portion of the Los Angeles segment also corresponds to a region where the tip of the thrust ramp, and the overlying kink band, are situated at the base of the broad monoclinal panel that forms the northern border of the central Los Angeles basin (Schneider *et al.*, 1996). Perhaps the southeast strike of this portion of the PHT was inherited from the trend of the preexisting monocline.

Quaternary Slip and Slip Rates

Quaternary slip on the PHT forms the discrete forelimb kink bands and produces structural relief of Quaternary strata above the three major thrust ramp segments (Fig. 9). As the fault system is blind and does not offset the base Quaternary horizon, we are unable to constrain fault slip by mapping stratigraphic offset. Thus, we employ two other

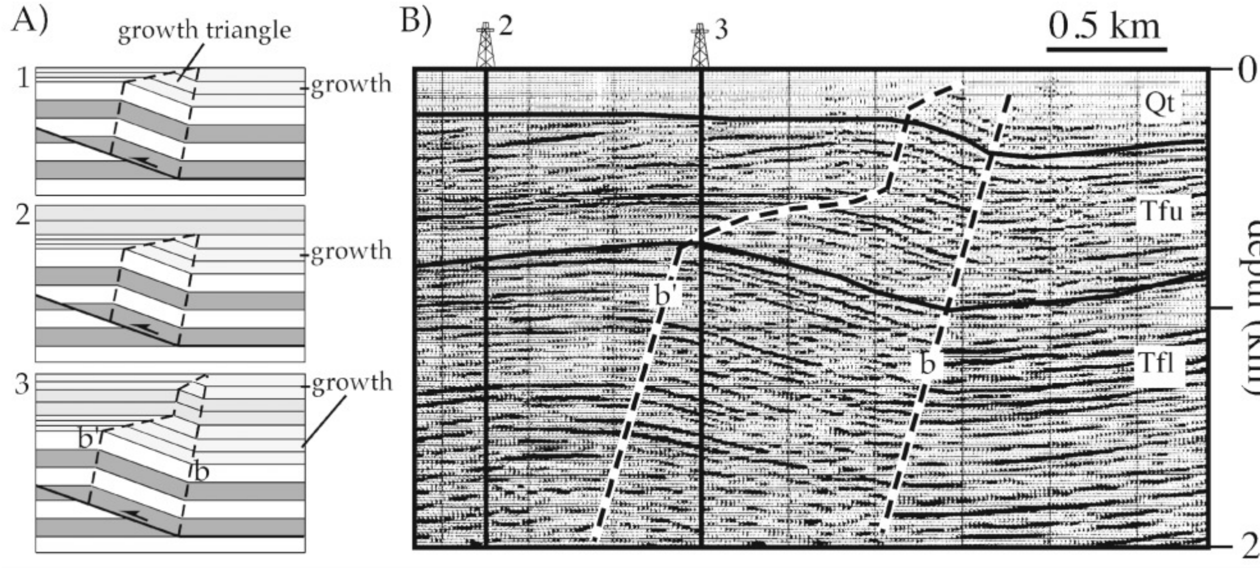

Figure 6. (A) Sequential kinematic model describing the evolution of a growth fault-bend fold (Suppe *et al.*, 1992). In model 1, slip across a synclinal fault bend produces a kink band that narrows upward in growth section (growth triangle). Model 2 depicts a period of deposition without fault motion. Model 3 shows reactivation of the fault, which extends the growth triangle upward into the shallow growth section. The reactivation history of the fault is recorded by inflections in the kink band's inactive axial surface (b′), which along with the active axial surface (b) bounds the growth triangle. (B) Depth-converted portion of the seismic profile in Figure 3 that images the backlimb growth triangle above the Santa Fe Springs fault segment. Inflections in the inactive axial surface (b′) are comparable to those modeled in A3 and record folding related to Pliocene activity, late Pliocene quiescence, and Quaternary reactivation of the underlying PHT. Formation symbols and wells identified in caption for Figure 3.

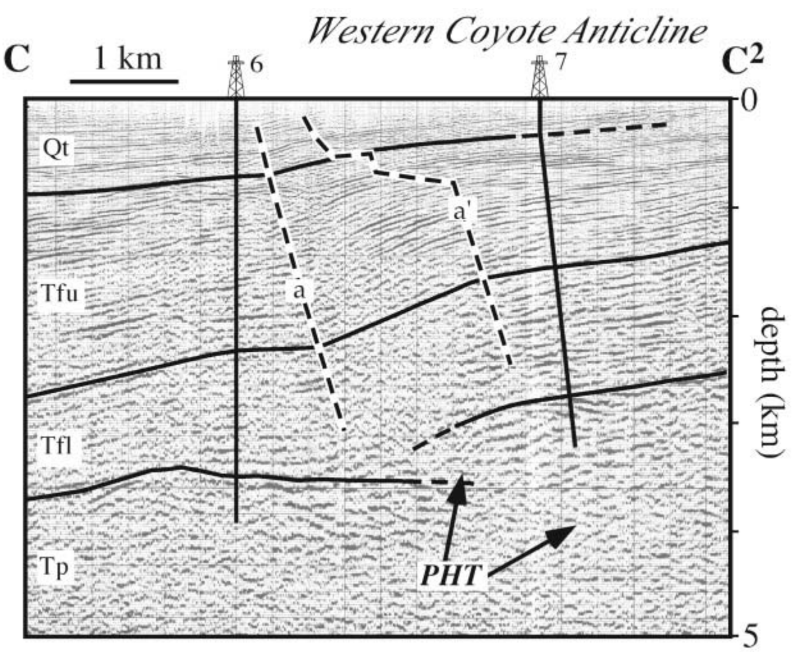

Figure 7. Migrated and depth-converted seismic reflection profile across the Coyote Hills segment of the PHT. The fault position is interpreted based on the downward termination of kink band aa′, reflection truncations, and structural relief of the Miocene and Pliocene strata. The fault terminates upward into the kink band (aa′), which narrows upward in Pliocene and Quaternary strata. Section trace is shown in Figure 1; stratigraphic nomenclature is described in Figure 3. Wells: 6, Chevron Rivera Community #1; 7, Westestates Santa Fe Springs #1.

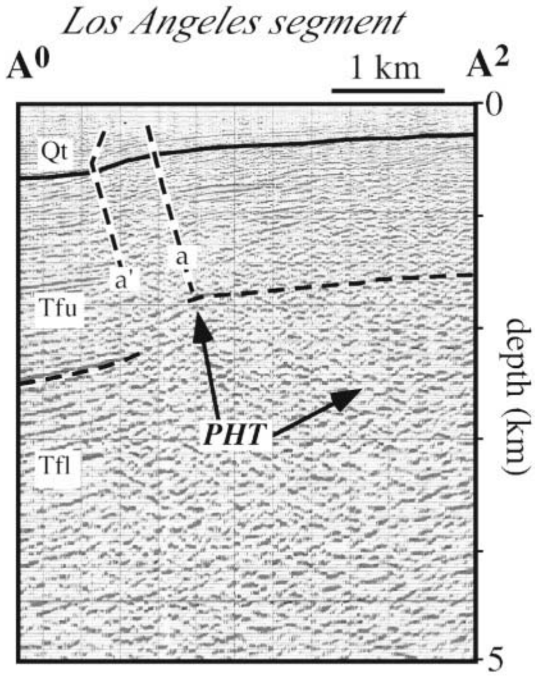

Figure 8. Migrated and depth-converted seismic reflection profile across the LA segment of the PHT. The fault position is interpreted based on the downward termination of kink band aa′, reflection truncations, and structural relief of the Miocene and Pliocene strata. Section trace is shown in Figure 1; stratigraphic nomenclature is described in Figure 3. Stratigraphic horizons are correlated from well control along the profile from the south.

techniques to map fault displacement. The first method uses measures of total structural relief across the anticlinal forelimb and the fault dips to calculate reverse slip (Fig. 10A). This method is straightforward, yet can be affected by primary sedimentary dip and cannot be used to distinguish whether a single or multiple thrust ramps contribute to the uplift. The second method (Fig. 10B) uses a measure of the width of the forelimb kink band as a measure of fault slip (Shaw and Suppe, 1994, 1996). Most kinematic models of fault-related folding imply some relation between kink-band width and fault slip; however, the conversion between these properties is specific to the kinematic model. For example, in fault-bend folds, including some classes of wedge structures, forelimb width is generally within 20% of fault dip slip (Suppe *et al.*, 1992) and can be calculated more precisely if fault orientation is known (Suppe, 1983).

Structural relief and kink-band widths were measured above the three ramp segments, with only the eastern portion of the Coyote segment omitted due to a lack of sufficient data. The fold width and uplift measurements track closely, generally being within 10% of one another (Fig. 11A). The similar shapes of the profiles imply that both kink-band width and uplift measurements reflect slip. We convert these measurements to fault slip estimates based on the following considerations. Structural relief is converted to maximum and minimum dip slip based on the minimum and maximum fault dip values (20° and 40°), respectively (Fig. 11B). This conservative fault-dip range takes into account all of the dip values observed on the seismic reflection data and the uncertainties in the velocity model used to depth convert the seismic sections. In order to calculate these maximum and minimum dip-slip values, we assume that uplift across the fold is equal to the fault heave. The conformable geometry of upper Pliocene pregrowth units across the fold crest observed in the seismic data (Figs. 2, 3) supports this assumption. The stratal geometry also implies that primary sedimentary dip did not significantly influence the structural relief measurement.

Using the same method, we calculated preferred slip values for the three fault segments (Fig. 11B) using a 27° N dip value. This dip value is based on the average ramp dip observed in the seismic data on all three segments and the linkage of the Santa Fe Springs segment to the 1987 Whittier Narrows (M_w 6.0) mainshock (Shaw and Shearer, 1999). Taking into account the uncertainty in the hypocentral location, we estimate that this dip value is correct within ±2° for the central portion of the Santa Fe Springs segment.

To evaluate the alternative slip estimation method, we converted the forelimb kink-band width of the Santa Fe Springs structure to slip using the fault dip value of 27°. The conversion is based on our interpretation of the forelimb kink-band at Santa Fe Springs as a fault-bend fold (Suppe, 1983). The fold kinematics are poorly constrained on the Coyote Hills and Los Angeles segments, so we did not consider these faults in this analysis. Fault-bend fold theory defines the ratio of slip (R) on the upper detachment and the fault ramp. Slip on the upper detachment is equal to kink-band width. For a 27° ramp dip, R is 0.73. The slip profile based on kink-band width tracks closely with the slip estimate based on uplift, reaching a maximum in the center of the trend and decreasing toward both segment boundaries (Fig. 11B). However, the slip derived from kink-band width generally underestimates the slip based on structural relief by about 25% for the same ramp dip. Underestimation of slip based on the kink-band width may reflect the fact that this method only considers slip that passes over the fault bend. Thus, it does not account for slip on the ramp that may be consumed by the broad anticlinal warping of the hanging wall (Figs. 3, 6, 7), which is taken into account by the slip calculation based on the total uplift.

All of the slip profiles exhibit patterns with maximum slip near the center of the fault segments (Fig. 11B). Slip tapers off toward the segment boundaries. Overlapping slip profiles across the segment boundaries imply that the fault segments are en echelon, meaning that they overlap one another along the north–south transport direction. The slip profiles suggest that slip is gradually transferred from one segment to the next. This slip pattern and fault geometry are consistent with a soft linkage among the ramp segments (Fig. 12A).

The fault-slip estimates can be used to calculate aver-

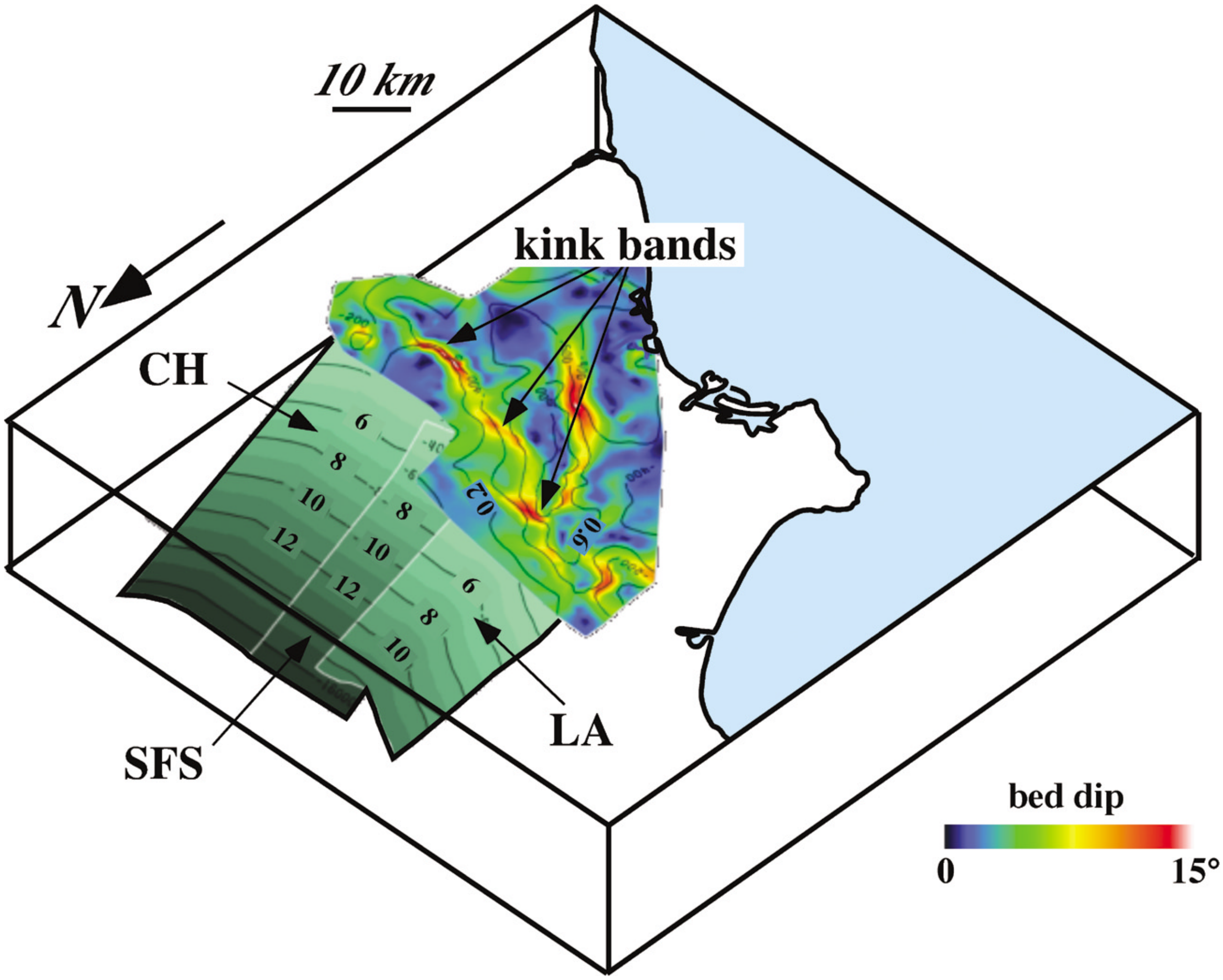

Figure 9. Perspective view of a three-dimensional model of the PHT and the overlying base Quaternary stratigraphic surface. The base Quaternary surface is folded by motion on the PHT, as reflected by the band of steep bed dips (color coded) in the forelimb kink bands. Contours are in kilometers subsea. CH, Coyote Hills segment; SFS, Santa Fe Springs segment; LA, Los Angeles segment.

age, long-term slip rates given the age of the sequence boundary that marks the initiation of Quaternary fold growth (Fig. 2). The base Quaternary horizon marks a transition from Quaternary nonmarine to Pliocene inner neritic strata. The boundary locally corresponds with the base of the La Habra sequence and the top of the Wheelerian benthic foraminiferal stage and is widely reported in oil wells (Blake, 1991; Wright, 1991). The precise age of this sequence boundary is not known, so we use an estimate of the maximum age of the top Wheelerian stage (1.6 Ma) (Blake, 1991) to make conservative slip-rate estimates. Based on this age, we calculate long-term slip rates on the portion of each PHT segment that has the greatest total slip. Ranges are provided based on the slip calculated using measured uplift and the minimum (20°) and maximum (40°) fault-dip values. The preferred rate is based on a 27° fault dip. For the Santa Fe Springs segment, the range of slip rates is 0.44–0.82 mm/yr, with a preferred rate of 0.62 mm/yr. The slip rate estimate for the Los Angeles segment is 0.60–1.13 mm/yr, with a preferred rate of 0.85 mm/yr. The Coyote segment has a faster slip rate, ranging from 0.90 to 1.70 mm/yr with a preferred rate of 1.28 mm/yr. These slip rates imply that the PHT accounts for 10%–25% of the shortening across the northern Los Angeles basin measured by geodesy (Argus *et al.*, 1999; Bawden *et al.*, 2001).

Systematic Behavior of the PHT Segments

Our geometric modeling and fault-slip analysis provide insights into the systematic behavior of the PHT. The three main segments of the PHT form an en echelon set of thrust ramps, with two major geometric segment boundaries separating the three fault ramps (Fig. 1). Slip appears to have initiated on all three fault segments in the early Quaternary (Fig. 2) based on the forelimb growth structures. The defined slip patterns mimic the observed uplift and kink-band widths

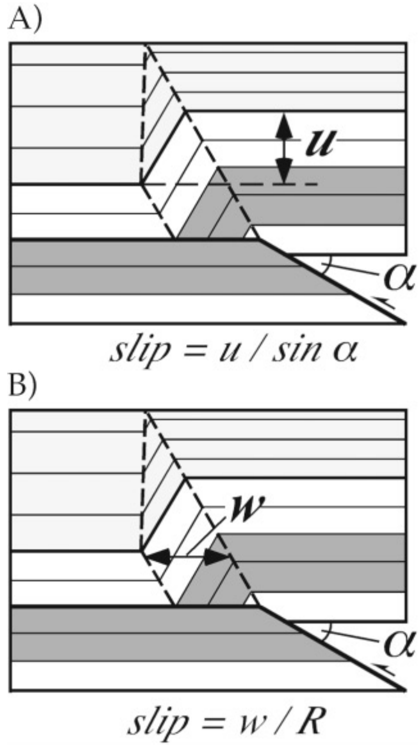

Figure 10. Fault-related fold models describing two methods of estimating fault slip. (A) Fault dip slip is derived from structural relief (u) and fault dip (α). (B) Fault dip slip is derived from kink-band width (w) and fault dip (α) using a conversion factor (R) derived from applicable fault-related folding theories.

and imply that slip is greatest near the center of each segment and decreases toward the segment boundaries (Fig. 11). Overlapping slip zones at the segment boundaries imply that displacement is transferred from one ramp segment to the next in an en echelon manner (Fig. 12A), rather than by a discrete tear fault (Fig. 12B). As slip decreases on one segment, slip on the adjacent segment increases. This soft-linkage pattern implies that thrust ramps overlap one another along the transport direction, which is consistent with the mapped fault surfaces (Fig. 1).

The measured uplift and kink band width on the three fault segments suggests that slip on the Santa Fe Springs segments is less than slip on the Los Angeles and Coyote segments (Fig. 11). This may be due to the presence of the south-dipping Montebello thrust (Figs. 1, 5), which lies north of the Santa Fe Springs fault segment. The Montebello thrust must intersect the Santa Fe Springs thrust ramp at depth and is either offset by the PHT or merges with it, forming a structural wedge (Medwedeff, 1992). In the latter scenario, slip on the PHT is partitioned between the south-dipping Montebello thrust fault and the north-dipping Santa Fe Springs ramp (Fig. 5). Thus, slip on the Santa Fe Springs ramp that we measured could be less than slip on the deeper portion of the PHT that lies north of its intersection with the Montebello thrust. As the Montebello backthrust is limited to the Santa Fe Springs segment, slip calculated on the Coyote and Los Angeles segments should reflect directly motion on the PHT at depth.

Slip appears to decrease to the west on the Los Angeles fault segment (Fig. 11). This may reflect oblique slip on the northwest–southeast trending portion of the Los Angeles fault segment (Fig. 1), leading to less dip slip in the west. Alternatively, or in addition, the Los Angeles segment of the PHT may have propagated to the west during the Quaternary, leading to less total slip on the western reaches of the fault system.

PHT in Relation to Other Faults in the Northern Los Angeles Basin

In addition to the PHT, the northern Los Angeles basin is deformed by several other large blind-thrust and strike-slip fault systems. We briefly summarize the relation of the PHT to these other fault systems because these relationships are critical for seismic hazard assessment.

The northern Los Angeles basin is located at the juncture of the Transverse and Peninsular Range Provinces and therefore contains both east–west and northwest–southeast structural trends. East–west trending structures are generally associated with the Transverse Range Province; whereas, northwest–southeast trending faults are ascribed to the Peninsular Range Province. The PHT represents the southernmost of the east–west trending fault systems, and thus we consider it to be the southern limit of the Transverse Ranges Province. Several other blind-thrust systems lie to the north and in the hanging wall of the PHT (Fig. 13, 14). These include the Las Cienegas and San Vicente faults (Wright, 1991; Schneider *et al.*, 1996), the (upper) Elysian Park thrust as described by Oskin *et al.* (1999), and the Santa Monica fault (Wright, 1991; Dolan *et al.*, 1995, 2000; Tsutsumi *et al.*, 2001). This part of the basin is also deformed by active, east to east–northeast trending strike-slip systems, including the Hollywood and Raymond faults (Dolan *et al.*, 1995, 1997; Walls *et al.*, 1998). The Cienegas fault (Schneider *et al.*, 1996) intersects the Los Angeles segment of the PHT at a depth of about 5 km. Thus, the Cienegas fault either merges with, or is offset by, the PHT. The Cienegas fault was active in the Pliocene but exhibits little or no evidence for Quaternary motion (Schneider *et al.*, 1996). This suggests that the younger PHT may have cut, and consequently rendered inactive, the Las Cienegas fault in the early Quaternary. None of the other major thrust faults in the northern basin intersect the PHT at shallow depths.

Several northwest–southeast trending fault systems associated with the Peninsular Range Province also occupy the northern Los Angeles basin. These structures include the (lower) Elysian Park thrust (EPT) (Davis *et al.*, 1989; Shaw and Suppe, 1996), the Anaheim Nose (Wright, 1991), and the Newport–Inglewood and Whittier strike-slip systems (Fig. 13). The lower EPT was inferred from the presence of a large, deeply rooted monoclinal fold panel that forms the

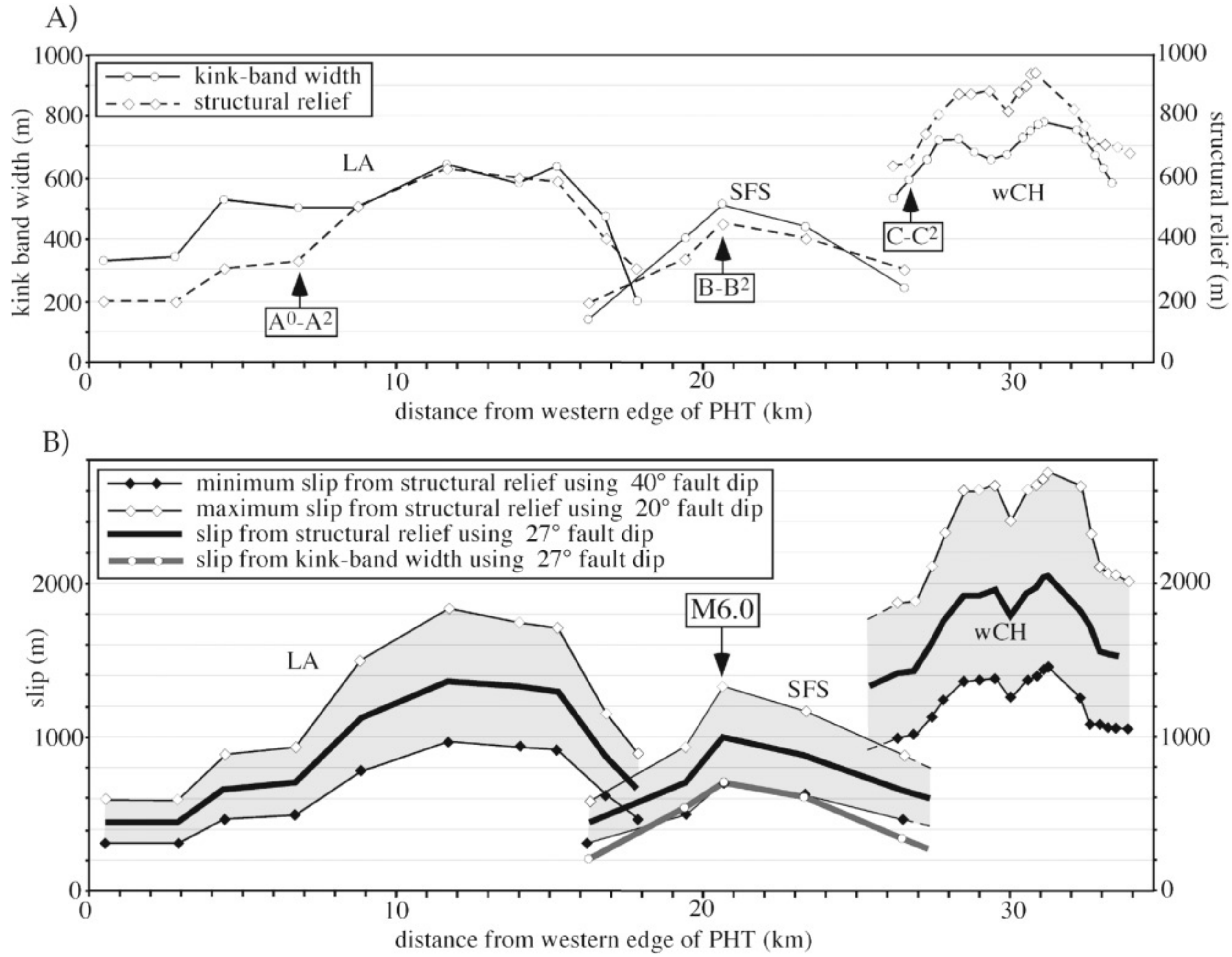

Figure 11. (A) Plot of kink-band width and structural relief measured from depth converted seismic profiles across the forelimbs that overlie the PHT. A^0–A^2, B–B^2, and C–C^2 denote positions along the profiles corresponding to the seismic sections presented in Figures 2, 3, 7, and 8. (B) Structural relief and kink-band width converted to slip using the methods described in Figure 10 and preferred (27°) and conservative (20 to 40°) fault-dip estimates.

northern border of the central Los Angeles basin. The Los Angeles and Santa Fe Springs segments of the PHT extend across, and offset, the upper portion of this fold trend (Fig. 3). Thus, the PHT lies above the lower Elysian Park thrust (Figs. 13, 14). The two fault ramps also have different strikes and slip histories (Davis *et al.*, 1989; Shaw and Suppe, 1996). This implies that the PHT and lower EPT are distinct fault systems and must be considered as separate potential earthquake sources.

The Whittier fault system extends across the Santa Fe Springs and Coyote Hills segments of the PHT (Fig. 13). The largest aftershock (local magnitude [M_L] 5.3) of the 1987 Whittier Narrows earthquake had a right-lateral, strike-slip focal mechanism (Hauksson and Jones, 1989). Based on the relocated aftershock cluster (Shaw and Shearer, 1999), it appears that this event occurred on a northwestern splay of the Whittier fault system (Fig. 13), perhaps the East Montebello fault (Wright, 1991). This secondary rupture was limited to the hanging wall of the Santa Fe Springs segment of the PHT, which extends downdip beneath the ruptured splay of the Whittier fault (Fig. 5). Thus, the strike-slip fault is either limited to the hanging wall of the PHT or is offset at depth by the thrust with displaced hanging-wall and footwall segments. Both scenarios imply that these two major fault systems are in contact within the seismogenic crust and, therefore, may have linked slip and rupture histories.

Regional Earthquake Hazards

The PHT extends for more than 40 km across the northern LA basin and directly underlies the downtown area (Fig. 1). The 1987 Whittier Narrows M_w 6.0 earthquake and folded late Quaternary deposits above the fault tip line (Fig. 4) demonstrate that the fault is active. The deformation im-

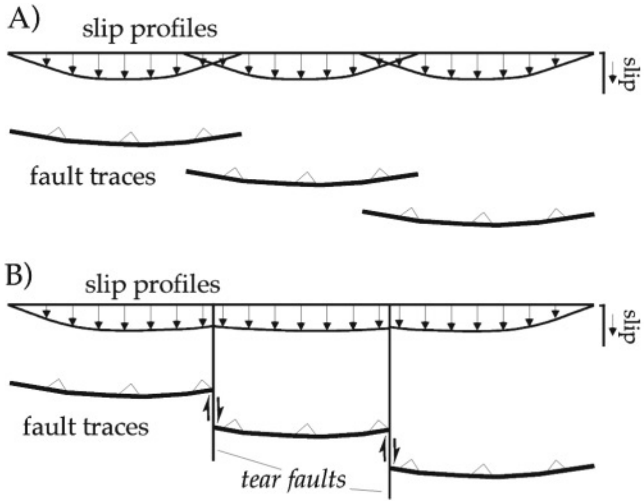

Figure 12. (A) Schematic, map-view slip profiles and fault traces diagnostic of a soft-linkage style of thrust segmentation. The fault traces overlap in an en echelon manner, and slip is gradually transferred from one fault segment to the next. (B) Schematic, map-view slip profiles and fault traces diagnostic of a hard-linkage style of thrust segmentation. The thrust traces terminate into tear faults, which abruptly transfer slip from one thrust segment to the next.

aged in the high-resolution seismic reflection data (Pratt *et al.*, 2002) also imply that past earthquakes have produced discrete folds at the Earth's surface (King and Vita-Finzi, 1981), similar to structures developed during the 1999 Chi Chi (M_w 7.7) earthquake in Taiwan (Suppe *et al.*, 2000). As discrete surface folding of this type did not occur during the 1987 M_w 6.0 event, we suggest that larger earthquakes capable of near-surface folding have occurred on the PHT in the past. These events may have been single or multisegment ruptures of the PHT (Shaw and Shearer, 1999). To estimate the sizes of these earthquakes, we calculate the area of the fault ramps between 5- and 17-km depth and use empirical relations that relate rupture area to earthquake magnitude (Wells and Coppersmith, 1994). The three fault surfaces have areas of 370 (Los Angeles), 260 (Santa Fe Springs), and 380 (Coyote) km^2. Based on the en echelon, soft-linkage nature of PHT fault segments (Fig. 12A) and the separation of the fault ramps at depth (Fig. 1), it seems possible that the fault segments can rupture independently. If these segments ruptured completely in separate earthquakes, the Los Angeles and Coyote segments would produce M_w 6.6 earthquakes and the Santa Fe Springs segment would produce a M_w 6.5 earthquake. These single segment earthquakes may occur in closely spaced sequences. This behavior has been well documented in a similar en echelon blind-thrust system in central California, which ruptured in the 1981 New Idria (M_w 5.4), 1983 Coalinga (M_w 6.5), and 1985 Kettleman Hills (M_w 6.1) earthquake sequence (Stein and Ekstrom, 1992). The similar fault geometries, slip rates, and slip histories of the three PHT segments, however, suggest that large multisegment ruptures are also possible. Simultaneous rupture of all three PHT segments would produce a M_w 7.1 earthquake.

Based on the average Quaternary fault-slip rates and empirical estimates of coseismic displacement for thrust earthquakes (Wells and Coppersmith, 1994), we calculate the average repeat times for our single and multisegment rupture scenarios. The range of repeat times for a given earthquake scenario are based on the range of fault-slip rates. Single-segment (M_w 6.6) ruptures on the Los Angeles and Coyote segments have average repeat times of 540–1000 years and 400–600 years, respectively. Earthquakes limited to the Santa Fe Springs segment (M_w 6.5) would rupture every 720–1320 years. Average repeat time on the Santa Fe Springs segment may be more similar to those on the other segments if the Montebello thrust branches from the PHT and consumes slip, as discussed previously. Potential M_w 7.1 multisegment ruptures would occur less frequently, with a repeat time of 780–2600 years. Single or multisegment earthquakes would cause extensive damage to metropolitan Los Angeles (Heaton *et al.*, 1995) based on the experience of the 1994 Northridge (M_w 6.7) earthquake (Scientists of the U.S. Geological Survey [USGS] and Southern California Earthquake Center [SCEC], 1994). The Northridge earthquake occurred on a blind-thrust fault beneath a northern suburb of Los Angeles and was similar in source type and magnitude to the single-segment earthquake scenarios proposed for the PHT. The Northridge event caused more than $40 billion dollars in property damage (Eguchi *et al.*, 1998). The PHT represents three potentially independent sources capable of generating similar earthquakes directly beneath metropolitan Los Angeles.

Conclusions

Over the past two decades, scientists have debated the existence and earthquake potential of blind-thrust faults beneath LA. The PHT offers the first compelling image of an active, seismogenic blind-thrust fault beneath metropolitan Los Angeles, confirming that such faults pose credible earthquake hazards. The fault is imaged in seismic reflection profiles acquired by the petroleum industry and is considered the source of the 1987 Whittier Narrows (M_w 6.0) earthquake (Shaw and Shearer, 1999). The fault comprises three distinct fault segments that extend beneath metropolitan Los Angeles. Each segment is overlain by a discrete forelimb kink band. These kink bands were imaged by industry and high-resolution seismic data and extend from about 3-km depth to the shallow subsurface ($<$15 m) where they deform late Quaternary strata. These observations confirm that the PHT is active and imply that it is capable of generating large earthquakes that produce surface fold scarps.

We applied two methods to estimate Quaternary fault displacement on the PHT, one based on uplift and the other based on fold-limb (kink-band) width. Both methods yielded slip profiles that are greatest in the center of each segment

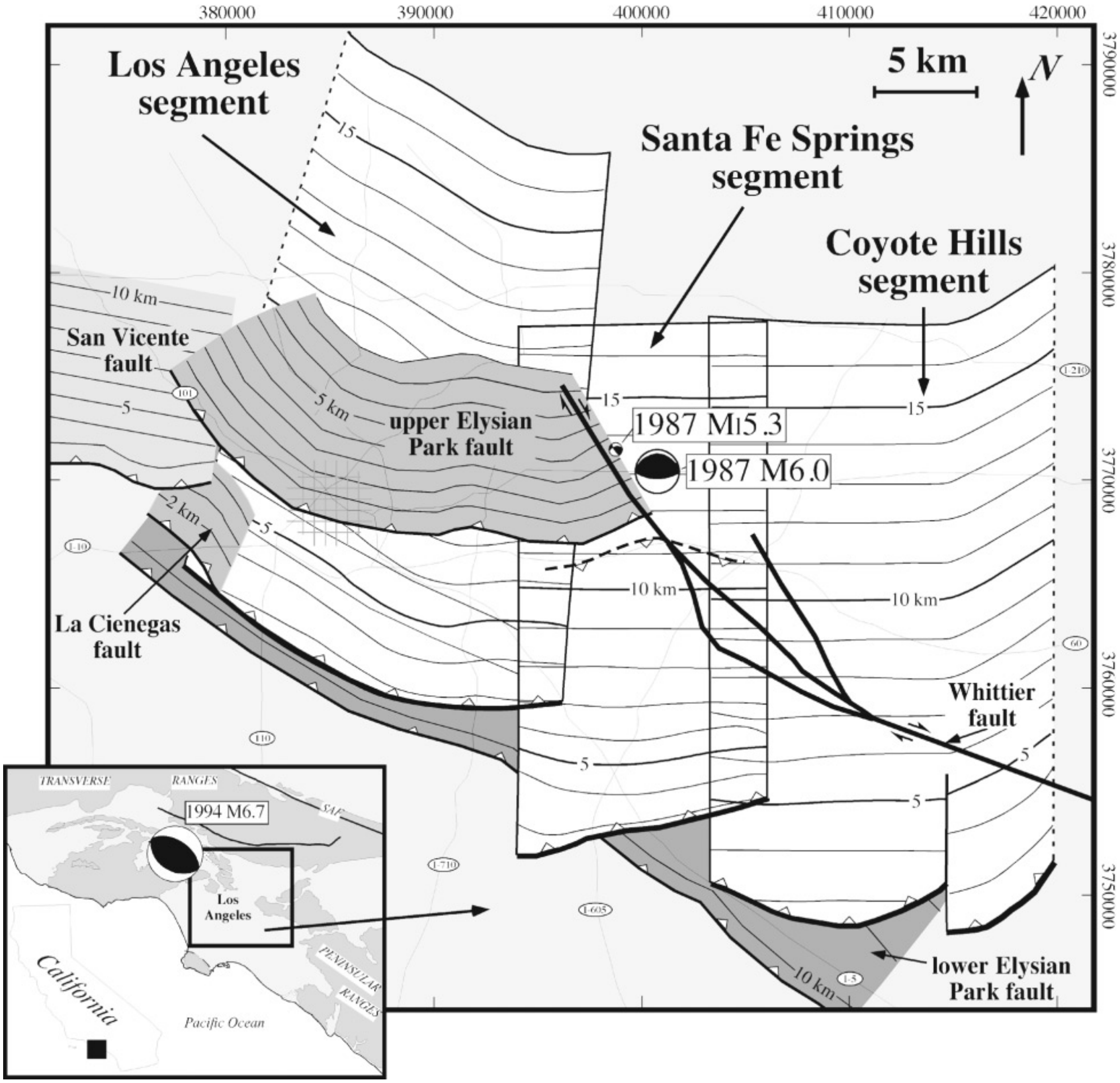

Figure 13. Structure contour map of the PHT in relation to other major thrust and strike-slip systems in the northern LA basin. Contour interval is 1 km; depths are subsea. Map coordinates are UTM Zone 11, NAD27 datum.

and that decrease toward the segment boundaries. These slip profiles, combined with the mapped fault geometry, imply that the PHT contains soft-segment boundaries. Soft-segment, or en echelon, fault systems are characterized by ramps that overlap along the transport direction and by displacement profiles in which slip is gradually transferred from one segment to another across the segment boundaries. The nature of these segment boundaries and the sizes of the fault ramps suggest that the PHT segments could rupture separately in M_w 6.5–6.6 earthquakes. Alternatively, these segments could rupture in larger, multisegment (M_w 7.1) earthquakes.

We calculated long-term average slip rates for each segment of the PHT based on the fault-slip estimates and an estimate of the age of thrust initiation in the early Quaternary. Slip rates range from 0.44 to 1.7 mm/yr, with preferred rates of 0.85, 0.62, and 1.28 mm/yr on the Los Angeles, Santa Fe Springs, and Coyote segments, respectively. These rates imply that the PHT accounts for 10% to 25% of the shortening across the northern Los Angeles basin that is measured by geodesy (Argus *et al.*, 1999; Bawden *et al.*, 2001). These slip rates suggest that, on average, single segment earthquakes (M_w 6.5–6.6) could occur on each segment about every 400 to 1320 years; whereas, multisegment (M_w

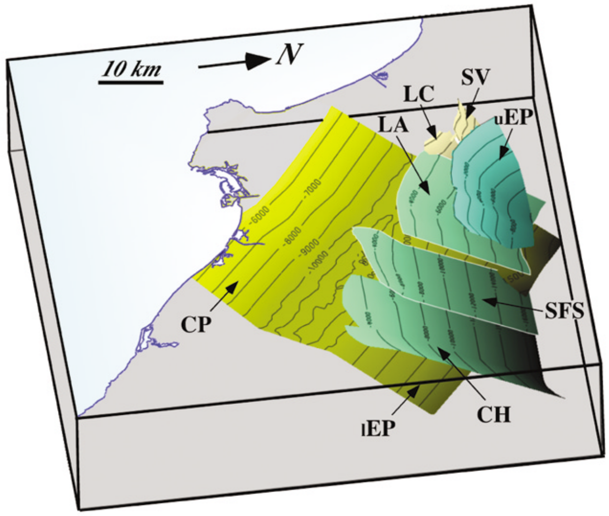

Figure 14. Perspective view of a three-dimensional model describing the PHT in relation to other major blind-thrust systems in the northern Los Angeles basin. PHT segments: CH, Coyote Hills; SFS, Santa Fe Springs; LA, Los Angeles segment; SV, San Vicente fault; LC, Las Cienegas fault (Schneider *et al.*, 1996); uEP, upper Elysian Park thrust (Oskin *et al.*, 2000); lEP, lower Elysian Park (Davis *et al.*, 1989; Shaw and Suppe, 1996); CP, Compton ramp (Shaw and Suppe, 1996).

7.1) earthquakes could occur with repeat times of 780–2600 years. As shown by the 1994 Northridge (M_w 6.7) event, earthquakes of these magnitudes would cause severe damage in the LA metropolitan area.

Acknowledgments

This research was supported by the National Earthquake Hazards Reduction Program (Grant 01HQGR0035), SCEC, and the National Science Foundation (EAR-0087648). The authors thank Michelle Cooke, Karl Mueller, Tom Rockwell, and Tom Wright for their helpful insights and John Suppe and Robert S. Yeats for constructive reviews.

References

Allmendinger, R. W. (1998). Inverse and forward numerical modeling of trishear fault-propagation folds, *Tectonics* **17,** 640–656.

Allmendinger, R., and J. H. Shaw (2002). Estimation of fault-propagation distance from fold shape: implications for earthquake hazards assessment, *Geology* **28,** no. 12, 1099–1102.

Argus, D. F., M. D. Heflin, A. Donnellan, F. H. Webb, D. Dong, K. J. Hurst, D. C. Jefferson, G. A. Lyzenga, M. M. Watkins, and J. F. Zumberge (1999). Shortening and thickening of metropolitan Los Angeles measured and inferred by using geodesy, *Geology* **27,** 703–706.

Bawden, G. W., W. Thatcher, R. S. Stein, K. W. Hudnut, and G. Peltzer (2001). Tectonic contraction across Los Angeles after removal of groundwater pumping effects, *Nature* **412,** 812–815.

Barbier, M. G. (1983). *The Mini-Sosie Method*, International Human Resources Development Corporation, Boston, 186 pp.

Blake, G. H. (1991). Review of Neogene biostratigraphy and stratigraphy of the Los Angeles basin and implications for basin evolution, in *Active Margin Basins*, K. T. Biddle (Ed.), American Association of Petroleum Geologists Memoir 52, 135–184.

Davis, T. L., J. Namson, and R. F. Yerkes (1989). A cross section of the Los Angeles area: seismically active fold-and-thrust belt, the 1987 Whittier Narrows Earthquake and earthquake hazard, *J. Geophys. Res.* 94, 9644–9664.

Dolan, J. F., K. Sieh, T. K. Rockwell, R. S. Yeats, J. Shaw, J. Suppe, G. Huftile, and E. Gath (1995). Prospects for larger or more frequent earthquakes in the greater Los Angeles metropolitan region, California, *Science* **267,** 199–205.

Dolan, J. F., K. Sieh, T. K. Rockwell, P. Guptill, and G. Miller (1997). Active tectonics, paleoseismology, and seismic hazards of the Hollywood fault, northern Los Angeles basin, California, *Geol. Soc. Am. Bull.* **109,** 1595–1616.

Dolan, J. F., K. Sieh, and T. K. Rockwell, (2000). Late Quaternary activity and seismic potential of the Santa Monica fault system, Los Angeles, California, *Geol. Soc. Am. Bull.* **112,** 1559–1581.

Eguchi, R. T., J. D. Goltz, C. E. Taylor, S. E. Chang, P. J. Flores, L. A. Johnson, H. A. Seligson, and N. C. Blais (1998). Direct economic losses in the Northridge earthquake: a three-year post-event perspective, *Earthquake Spectra* **14,** 245–264.

Erslev, E. A. (1991). Trishear fault-propagation folding, *Geology* **19,** 617–620.

Hauksson, E. (1990). Earthquakes, faulting and stress in the Los Angeles Basin, *J. Geophys. Res.* **95,** 15365–15394.

Hauksson, E., and L. M. Jones (1989). The 1987 Whittier Narrows Earthquake sequence in Los Angeles, southern California: seismological and tectonic analysis, *J. Geophys. Res.* **94,** 9569–9589.

Heaton, T. H., J. F. Hall, D. J. Wald, and M. W. Halling (1995). Response of high-rise and base-isolated buildings to a hypothetical M_w 7.0 blind-thrust earthquake, *Science* **267,** 206–210.

King, G. C. P., and C. Vita-Finzi (1981). Active folding in the Algerian earthquake of 10 October 1980, *Nature* **292,** 22–26.

Medwedeff, D. A. (1992). Geometry and kinematics of an active, laterally propagating wedge thrust, Wheeler Ridge, California, in *Structural Geology of Fold and Thrust Belts*, S. Mitra and G. Fisher (Eds.) John Hopkins University Press, Baltimore, 3–28.

Myers, D. J. (2001). Structural geology and dislocation modeling of the east Coyote anticline, Eastern Los Angeles basin, M.S. Thesis, Oregon State University, 49 pp.

Oskin, M., K Sieh, T. Rockwell, G. Miller, P. Guptill, M. Curtis, S. McArdle, and P. Elliot (2000). Active parasitic folds on the Elysian Park anticline: Implications for seismic hazard in central Los Angeles, California, *Geol. Soc. Am. Bull.* **112,** no. 5, 693–707.

Pratt, T. L., J. H. Shaw, J. F. Dolan, S. Christofferson, R. A. Williams, J. K. Odum, and A. Plesch (2002). Shallow folding imaged above the Puente Hills blind-thrust fault, Los Angeles, California, Geophys. Res. Lett. (in review).

Schneider, C. L., C. Hummon, R. S. Yeats, and G. Huftile (1996). Structural evolution of the northern Los Angeles basin, California, based on growth strata, *Tectonics* **15,** 341–355.

Scientists of the U.S. Geological Survey and the Southern California Earthquake Center (1994). The magnitude 6.7 Northridge, California, Earthquake of 17 January 1994, *Science* **266,** 389–397.

Shaw, J. H., and P. M. Shearer (1999). An elusive blind-thrust fault beneath metropolitan Los Angeles, *Science* **283,** 1516–1518.

Shaw, J. H., and J. Suppe (1994). Active faulting and growth folding in the eastern Santa Barbara Channel, California, *Geol. Soc. Am. Bull.* **106,** 607–626.

Shaw J. H., and J. Suppe (1996). Earthquake hazards of active blind-thrust faults under the central Los Angeles basin, California, *J. Geophys. Res.* **101,** 8623–8642.

Shearer, P. M. (1997). Improving local earthquake locations using the L1 norm and waveform cross correlation: Application to the Whittier Narrows, California, aftershock sequence, *J. Geophys. Res.* **102,** 8269–8283.

Stein, R. S., and G. Ekstrom (1992). Seismicity and geometry of a 110-km-long blind thrust fault, 2, Synthesis of the 1982–85 California Earthquake Sequence, *J. Geophys. Res.* **97,** 4865–4883.

Suppe, J. (1983). Geometry and kinematics of fault-bend folding, *Am. J. Sci.* **283,** 684–721.

Suppe, J., and D. A. Medwedeff (1990). Geometry and kinematics of fault-propagation folding, *Ecologae Geol. Helv.* **83,** no. 3, 409–454.

Suppe, J., G. T. Chou, and S. C. Hook (1992). Rates of folding and faulting determined from growth strata, in *Thrust Tectonics*, K. R. McClay (Ed.), Chapman Hall, London, 105–121.

Suppe, J., Y. H. Lee, Y. G. Chen, and J. H. Hung (2000). Coseismic fault-bend folding: Fold scarp formation in the 1999 Chi-Chi earthquake (M 7.6), Taiwan Fold-and-thrust belt, *EOS* **81,** no. 48, 874.

Süss, M. P., and J. H. Shaw (2003). *P*-wave seismic velocity structure derived from sonic logs and industry reflection data in the Los Angeles Basin, California, *J. Geophys. Res.* (in press).

Tsutsumi, H., R. S. Yeats, and G. J. Huftile (2001). Late Cenozoic tectonics of the northern Los Angeles fault system, California, *Geol. Soc. Am. Bull.* **113,** 454–468.

Walls, C., T. Rockwell, K. Mueller, Y. Bock, S. Williams, J. Pfanner, J. Dolan, and P. Feng (1998). Escape tectonics in the Los Angeles metropolitan region and implications for seismic risk, *Nature* **394,** 356–360.

Wells, D. L., and K. J. Coppersmith (1994). New empirical relationships among magnitude, rupture length, rupture width, rupture area, and surface displacement, *Bull. Seism. Soc. Am.* **84,** 974–1002.

Wright, T. L. (1991). Structural geology and tectonic evolution of the Los Angeles basin, California, in *Active Margin Basins*, K. T. Biddle (Ed.), American Association of Petroleum Geologists Memoir 52, 35–134.

Yerkes, R. F. (1972). Geology and oils resources of the western Puente Hills area, Southern California, *U.S. Geol. Surv. Profess. Pap. 420-C*, 63 pp.

Department of Earth and Planetary Sciences
Harvard University
20 Oxford St.
Cambridge, Massachusetts 02138
shaw@eps.harvard.edu
(J.H.S., A.P., P.F.)

Department of Earth Sciences
University of Southern California
Los Angeles, California 90089
(J.F.D.)

U.S. Geological Survey
Seattle, Washington 98115
(T.L.P.)

Manuscript received 16 November 2001.